Multiphonon-assisted tunneling through deep levels: A rapid energy-relaxation mechanism in nonideal quantum-dot heterostructures

Peter C. Sercel
Department of Physics and Materials Science Institute, University of Oregon, Eugene, Oregon 97403
(Received 28 December 1994)

The presence of a deep-level trap coupled to a quantum-dot heterostructure is shown to provide a rapid energy-relaxation pathway through which electrons may thermalize. A capture process is considered whereby a free conduction-band electron is captured into the ground conduction-band state of a quantum dot by multiphonon-assisted tunneling through the trap. As an example calculation, transition rates for a 5 nm radius $In_{0.5}Ga_{0.5}As/GaAs$ quantum dot coupled to the defect $M1$ are calculated as a function of separation between the quantum dot and the deep level. For separations less than $\approx$ 10 nm these rates are found to be in excess of 10^{10} s^{-1} at 4.2 K. The result suggests that the presence of point defects may serve to enhance the luminescence efficiency of quantum-dot material. The physical situation described in this paper could only arise if the spatial distribution of defects were strongly correlated with that of the quantum-dot structures, e.g., through formation of interface states or point defects as a consequence of the growth process. With this caveat, the proposed mechanism may possibly explain the failure to observe a significant phonon bottleneck effect in recent work on $In_{1-x}Ga_xAs$ quantum-dot structures [e.g., Appl. Phys. Lett. **64**, 2815 (1994)].

I. INTRODUCTION

Among the most interesting features of the behavior of zero-dimensional electronic systems, such as quantum-dot heterostructures, is the decoupling of the electrons from the phonon bath, which is predicted to occur when the level splittings exceed the optical phonon energy.[1–3] In this circumstance, energy relaxation by single phonon emission is suppressed, due to energy and momentum conservation requirements. This effect has come to be known as the phonon bottleneck.

In addition to the obvious fundamental interest in this problem, it is an important one from the standpoint of applications, since many proposed uses of quantum-dot structures, for example, as gain media in semiconductor lasers, naturally require rapid thermalization of electrons relative to the optical transition rate. In the case of conventional double heterostructure or quantum well lasers, internal equilibrium within a band is ensured by the rapidity of intraband carrier-carrier and carrier-phonon scattering, which occur with subpicosecond relaxation times. However, as has been recently pointed out by several authors,[1–5] in an ideal quantum-dot system the assumption of quasiequilibrium in the conduction band breaks down. Energy relaxation by emission of longitudinal-acoustic (LA) phonons was shown to be increasingly quenched with increasing energy level separation.[1] Single longitudinal-optical (LO) phonon emission, on the other hand, is forbidden except in the unlikely case that energy level separation equals $\hbar\omega_{LO}$.[1,2] Calculations extended to second order in the electron-phonon interaction indicate that a "window" of rapid relaxation may occur between quantum-dot states separated by energy $\hbar\omega_{LO} \pm \hbar\omega_{LA}$, where $\hbar\omega_{LO}$ and $\hbar\omega_{LA}$ are longitudinal-optical and -acoustic phonon energies, respectively.[3] While this result may provide a solution to the relaxation bottleneck problem for appropriately designed quantum dots, the requirement is a rather stringent one in that a ladder of states separated by roughly $\hbar\omega_{LO}$ is still required to span the gap between the barrier continuum and the ground state of the quantum dot. Other relaxation mechanisms which have been studied include intraband radiative transitions and Coulombic collisional deexitation processes.[4,5] The former process was shown to be slower than interband radiative recombination when the intraband level spacings are less than the bulk energy gap owing to the cubic dependence of the spontaneous emission rate on the transition energy. Collisional deexitation was found to be the dominant relaxation process at free carrier densities greater than 10^{16} cm^{-3} in a GaAs -$Al_xGa_{1-x}As$ quantum-dot system, but is insufficiently rapid to establish local thermal equilibrium below carrier densities of 10^{19} cm^{-3}.[4]

These calculations all share the feature that they consider ideal quantum-dot systems, and do not consider the influence of extrinsic deep level or interface states on the energy-relaxation process. Here, I describe a theoretical investigation of the effect of coupling between a deep-level state and a quantum dot. Owing to the strong lattice coupling in deep centers, deep-level traps may provide a rapid relaxation channel for carrier capture into deeply bound quantum-dot states. The situation may be described as a form of *intraband* nonradiative decay through multiphonon emission. To illustrate the effect, I present an illustrative calculation pertinent to recent experimental realizations of quantum-dot heterostructures. The physical situation described in this paper could only arise if the spatial distribution of defects is strongly cor-

0163-1829/95/51(20)/14532(10)/$06.00

related with that of the quantum-dot structures, e.g., through formation of interface states or point defects as a consequence of the growth process. With this caveat, the proposed mechanism may possibly explain the failure to observe a significant phonon bottleneck effect in recent work on $In_xGa_{1-x}As$ quantum-dot structures.[6–8] The main conclusion of the present analysis is that the presence of point defects may serve to *enhance* the luminescence efficiency of the quantum-dot material.

II. QUANTUM DOT COUPLED TO A DEEP LEVEL

We consider the model system depicted in Fig. 1 consisting of a spherical $In_xGa_{1-x}As$ quantum dot of radius R embedded in a GaAs matrix, coupled to a deep-level trap located a distance A from the center of the quantum dot. In the calculation described below, we will choose as a representative deep center the electron trap $M1$, which is commonly observed in n-type GaAs grown by molecular beam epitaxy under arsenic stabilized conditions.[9,10]

To simplify the discussion, we have chosen to study a quantum-dot possessing only two bound conduction-band states — $D0$, the ground state, and $D1$, a higher lying state. LO-phonon scattering between the ground conduction-band state of the quantum dot and the excited state or continuum states above the barrier is assumed to be suppressed, due to the bottleneck effect. On the other hand, the excited state $D1$ is considered to be sufficiently close to the top of the barrier that it is coupled to the continuum via LO phonon scattering processes — this state is assumed to be in thermal equilibrium with the conduction-band states above the barrier. Since the relatively large heavy-hole mass causes the spacing of bound valence-band states to be significantly smaller than in the conduction band, we assume the valence-band states to be thermalized and focus our discussion on the conduction band. The occupied deep level is assumed to lie in energy between the ground and excited states of the quantum dot. This situation is shown schematically in Fig. 2.

In what follows, we analyze processes whereby an electron is captured into the trap and subsequently makes a transition into the quantum-dot ground state by multiphonon-assisted tunneling. In Sec. II, we present a discussion of the relevant physics of deep levels, utilizing a semiclassical description based upon the use of the configuration coordinate diagram. We then develop expressions for the multiphonon-assisted tunneling rates as a function of temperature and the interaction, J, between the deep level and the bound conduction-band states of the quantum dot. This calculation is performed in a static regime in which the deep level is assumed to be fully relaxed prior to each transition. The implicit neglect of dynamic effects, which can occur in sequential transitions, causes an underestimate of transition rates. Our results, therefore, represent a lower estimate of the intraband relaxation rates. Numerical results for $In_xGa_{1-x}As$ quantum dots coupled to the deep level $M1$, a representative electron trap found in GaAs grown by molecular beam epitaxy (MBE), are presented in Sec. III. We find there that coupling to a deep level can result in relaxation times as short as 100 ps in quantum dots at liquid helium temperatures. We conclude with a discussion of mechanisms by which the situation described here might arise in experiments.

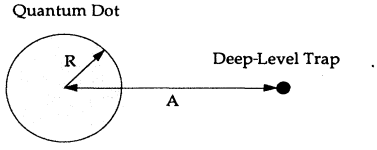

FIG. 1. Quantum dot in proximity to a deep-level trap. The separation between the quantum dot and the deep level is A.

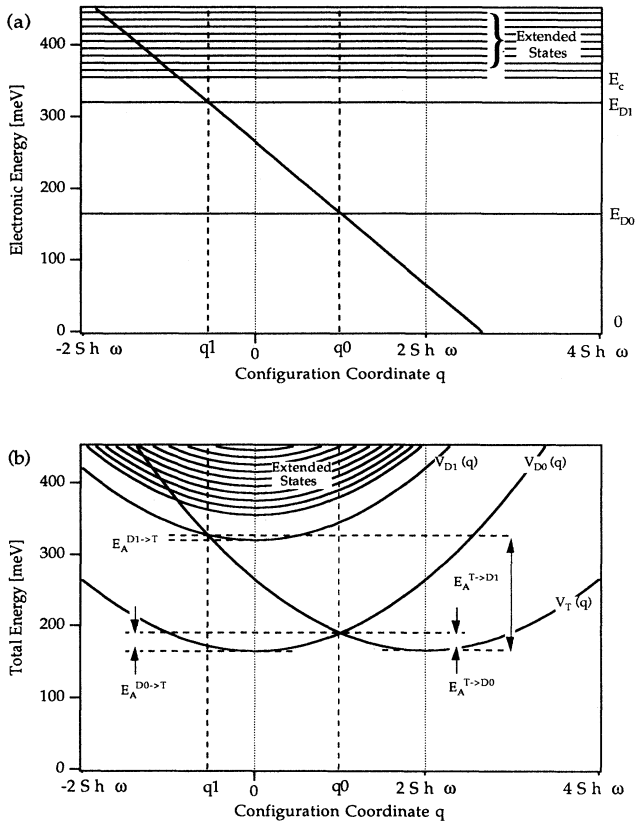

FIG. 2. Energy diagrams for the quantum dot and the deep level. (a) Electronic energy versus configuration coordinate, q. (b) Total energy (electronic plus elastic) versus configuration coordinate, q. Crossing points $q0$ and $q1$ are indicated in the figure.

A. Capture from the barrier into the trap

In the system shown in Fig. 1, initial capture of an electron into the trap can occur in two ways. The first

is by direct capture of electrons from the GaAs barrier. The other possibility is a two-step process involving LO-phonon mediated capture from the barrier into the excited state, $D1$, followed by multiphonon-assisted tunneling from $D1$ into the trap. The latter process will be discussed in Sec. II B. We now discuss the direct capture process.

The rate of capture, c, from the barrier directly into the trap may be readily calculated using the phenomenological capture cross section:

$$c = n\ v_{\rm th}\ \sigma. \tag{1}$$

Here n is the electron concentration in the GaAs barrier, $v_{\rm th}$ is the thermal velocity of electrons at temperature T, and σ is the capture cross section, which has the functional dependence on temperature given by[11]

$$\sigma = \sigma_\infty\ \exp\left[\frac{-E_B}{k_B T}\right], \tag{2}$$

where E_B is the capture barrier for the deep level in question.

B. Model of the deep level

The process of multiphonon-assisted tunneling between states in the quantum dot and the trap is somewhat more complicated, requiring a microscopic model of the trap in order to calculate overlap integrals, as well as a model for the electron-phonon coupling. For analytical simplicity, we model the trap potential well with a radial δ function, and calculate the electronic wave functions in the effective mass approximation. In this model the trap has a single electronic state, T, whose envelope function has the coordinate representation,

$$\langle\vec{\rho}|T\rangle = \psi_t(\vec{\rho}) = \left(\frac{\alpha}{2\pi}\right)^{\frac{1}{2}}\ \frac{e^{-\alpha\rho}}{\rho}. \tag{3}$$

The electronic energy associated with this state, measured with respect to the GaAs conduction-band edge, is

$$E_t = \frac{\hbar^2\alpha^2}{2m^*}. \tag{4}$$

This energy is strongly dependent on the local atomic configuration of the center. To model this coupling, we follow Henry and Lang[11] and take the energy to be a linear function of a configuration coordinate, Q, which describes the atomic displacement of the center:

$$E_t(Q) = E_0 - b\ Q. \tag{5}$$

Here, E_0 is the energy of the state when Q=0. When the trap state is unnoccupied, coordinate Q oscillates about zero with frequency ω. We assume that coupling between the electronic state and the lattice occurs through transverse-acoustic phonons, and model this process with a single frequency ω. When the trap is occupied, the configuration of the center distorts — Q shifts — so as to minimize the sum of electronic and elastic energy,

$$V_T(Q) = E_0 - bQ + \frac{M\omega^2 Q^2}{2}, \tag{6}$$

where M is a reduced mass associated with the center. The equilibrium position of the occupied trap, Q_T, is therefore given by

$$Q_t = \frac{b}{M\omega^2}. \tag{7}$$

The total energy — electronic plus elastic energy — of the occupied trap in its equilibrium position is conventionally written $E_T = E_0 - S\hbar\omega$, where S is the Huang-Rhys factor. Thus, the lattice relaxation energy written in terms of the configuration coordinate parameter is

$$S\hbar\omega = \frac{M\omega^2 Q_T^2}{2}. \tag{8}$$

Defining a renormalized configuration coordinate $q = bQ$, we can reexpress the electronic energy of the trap as

$$E_t(q) = E_0 - q, \tag{9}$$

and using 8, the *total* energy of the trap as a function of q assumes the form

$$V_T(q) = E_T + \frac{(q - 2S\hbar\omega)^2}{4S\hbar\omega}. \tag{10}$$

The latter two relations are plotted in Figs. 2(a) and 2(b), respectively, using parameters associated with the defect $M1$, discussed below in Sec. III. Also shown in Fig. 2(a) are the energies of the two bound conduction-band states in the quantum dot, E_{D0} and E_{D1}, as well as the energies of extended states with energy greater than E_c, the conduction-band edge in GaAs. In Fig. 2(b), total energy curves corresponding to these states are shown, representing states of the system when the trap is *unnoccupied.* These curves are described by the relations

$$V_i(q) = E_i + \frac{q^2}{4S\hbar\omega}. \tag{11}$$

Here, E_i represents the electronic energy with $i = D0, D1$ denoting the two bound states in the quantum dot. The parameters in Fig. 2 are calculated for a 5 nm radius $In_{0.5}Ga_{0.5}As$ quantum dot surrounded by GaAs, as described in Sec. III. We turn now to a discussion of the interaction between the quantum dot and the deep level.

C. Transitions between states of the quantum dot and the deep level

Referring to the configuration coordinate diagram of Fig. 2, it is clear that hopping between a state in the quantum dot and the deep level can occur only at points where the corresponding total energy curves cross. This is simply an expression of the Franck-Condon principle. We envision an initial condition in which an electron initially occupies one of these states. Coordinate q fluctuates so that at any time there is a finite probability for the system to pass through a crossing point. At that point, the interaction between the electronic wave functions of the deep level and the quantum dot may induce

a tunneling transition.

Henry and Lang[11] have developed a theory of capture from extended band states into deep levels by multiphonon emission, which has been successful in explaining the properties of many deep centers in III-V semiconductors. The capture process in such a case is nonadiabatic since the coupling between an extended state and the deep level is infinitesmal. In the present situation, however, we must consider coupling between two bound states where the coupling may be strong.

This situation has been analyzed by Sumi who studied energy transfer between localized electronic states strongly coupled to the lattice, and developed expressions for the transition rate as a function of coupling strength, bridging the adiabatic and nonadiabatic limits.[12–14] We follow Sumi in the analysis that follows.

Note that the crossing behavior at points $q1$ and $q0$ in Fig. 2(b) are distinct. This point is illustrated in Fig. 3, which shows the anticrossing behavior of the total energy curves for the two cases in the adiabatic (strong coupling) limit. In the ensuing discussion, we follow the terminology introduced by Sumi[12] and we refer to the situation obtaining at crossing point $q1$ as case I, while that at point $q0$ will be referred to as case II.

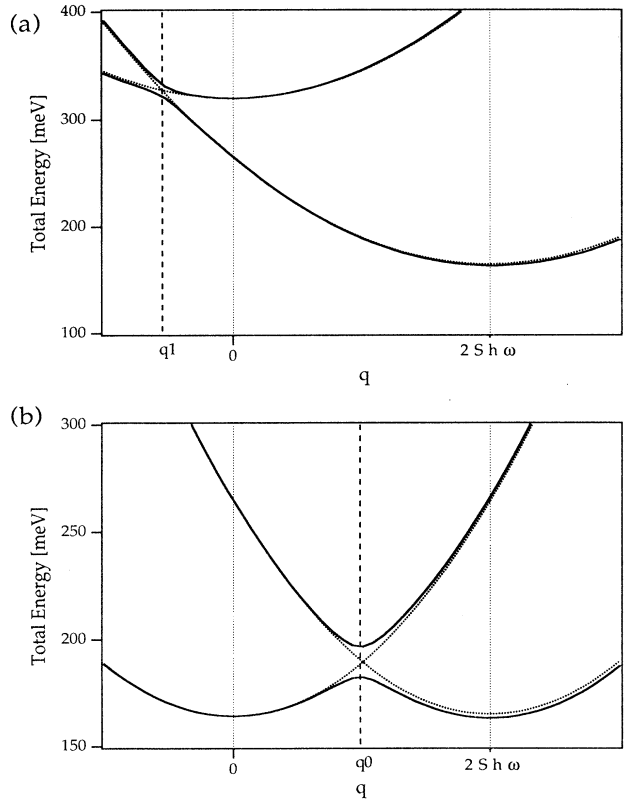

FIG. 3. Detail of the crossing points on the configuration coordinate diagram, Fig. 2(b). (a) Crossing point *q1*, corresponding to case I. (b) Crossing point *q0*, corresponding to case II. The solid lines depict the total energy curves in the adiabatic limit, $\gamma \gg 1$, where anticrossing behavior is expected. The dotted lines correspond to the weak coupling limit, $\gamma \ll 1$.

In both cases, during a *single* crossing the probability of electron transfer from one localized state i to the other, j, is given by the Landau-Zener crossing probability,[15]

$$1 - R = 1 - \exp\left[\frac{-2\pi J^2}{\hbar|v|}\right]. \tag{12}$$

In this expression, J is the interaction between the two localized states i, j, and $v = \frac{dq}{dt}$ is the velocity of the configuration coordinate at the crossing point. We will develop an expression for J in the next subsection. First, however, we derive expressions for the transition rates appropriate to case I and case II accounting for multiple crossing phenomena and the possibility of reemission.

1. *Transition rate through q1: Case I*

We now consider the total probability of crossing from the quantum-dot state $D1$ to the trap state T in a twofold passage through the crossing point $q1$, shown in Fig. 2(b), taking into account the possibility of reemission. In such a twofold passage, there are two ways that the electron might begin in $D1$ and end up in state T. The first is that the electron crosses during the first passage with probability $1 - R$ and remains in state T on the return trip through the crossing point with probability R. The second possibility is that the electron does not cross during the first passage (probability R), but does so in the second (with probability $1 - R$). Thus, the total probability of a transition during a twofold passage through the crossing point is

$$P = 2R(1 - R). \tag{13}$$

Using this, we can write an instantaneous transition rate given by

$$W^i = 2\ R[1 - R]\ v\theta(-v)\delta(q - q1). \tag{14}$$

In this expression, the first factor is simply the Landau-Zener crossing probability, while the factor of v represents the flux through the crossing point. The factor $\delta(q - q1)$ enforces the Franck-Condon principle, namely, that transitions can occur only at the crossing point $q1$, while the step function $\theta(-v)$ reflects the fact that the crossing from $D1$ to T is approached from the right in Fig. 2(b).

The transition rate at a given temperature is found by averaging W^i over the appropriate probability distribution functions for q and v. These distribution functions, for an oscillator in thermal equilibrium, are given by[16]

$$\rho(q) = \frac{1}{\sqrt{2\pi}\zeta_q} \exp\left[-\frac{(q - \bar{q})^2}{2\zeta_q^2}\right], \tag{15}$$

and

$$\rho(v) = \frac{1}{\sqrt{2\pi}\zeta_v} \exp\left[-\frac{v^2}{2\zeta_v^2}\right]. \tag{16}$$

Here, $\bar{q}$ denotes the thermal average of the configuration

coordinate, which in the present case is zero, since we are considering transitions from the quantum dot. The parameters ζ_q and ζ_v denote the mean square thermal fluctuation of q and v, given by the expressions[16]

$$\zeta_q^2 = (b\zeta_Q)^2 = b^2 \left(\frac{\hbar}{2M\omega}\right) \coth\left(\frac{\hbar\omega}{2k_BT}\right) \tag{17}$$

and

$$\zeta_v^2 = \omega^2 \zeta_q^2. \tag{18}$$

Using Eqs. (7) and (8), it is simple to reexpress ζ_q in terms of the experimentally accessible lattice relaxation energy, eliminating the unknown reduced mass M:

$$\zeta_q^2 = \hbar\omega \; S\hbar\omega \coth\left(\frac{\hbar\omega}{2k_BT}\right). \tag{19}$$

For later reference, we note here that in the high temperature limit $k_bT \gg \hbar\omega$ Eq. (19) takes the form[13]

$$\zeta_q^2 = 2S\hbar\omega k_BT. \tag{20}$$

Using Eqs. (14) and (15–19), we can now write an expression for the average transition rate, $W_I^{D1\to T}$ from $D1$ to T:[12]

$$W_I^{D1\to T} = \langle\langle \delta(q - q_1)\rangle\rangle_q \langle\langle 2vR[1-R]\theta(-v)\rangle\rangle_v, \tag{21}$$

where

$$\langle\langle f(q)\rangle\rangle_q = \int_{-\infty}^{+\infty} dq f(q)\rho(q) \tag{22}$$

and

$$\langle\langle f(v)\rangle\rangle_v = \int_{-\infty}^{+\infty} dv \; f(v) \; \rho(v). \tag{23}$$

After some algebra, the transition rate can be written

$$W_I^{D1\to T} = \frac{\omega}{2\pi} \; \eta_I \; \exp[-q_1^2/2\zeta_q^2]. \tag{24}$$

It is straightforward to show that the reverse rate, from T to $D1$, is given by

$$W_I^{T\to D1} = \frac{\omega}{2\pi} \; \eta_I(\gamma) \; \exp\left[-\frac{(q1 - 2S\hbar\omega)^2}{2\zeta_q^2}\right], \tag{25}$$

where ζ_q is defined by Eq. (19).

In these expressions, $\omega/2\pi$ may be interpreted as an attempt frequency, while η_I is an efficiency factor, which has the explicit form

$$\eta_I = \frac{\sqrt{2\pi}}{\omega\zeta_q} \; \langle\langle 2vR[1-R]\theta(-v)\rangle\rangle_v. \tag{26}$$

Introduction of a dimensionless adiabaticity parameter

$$\gamma = \frac{2\pi J^2}{\hbar\omega\zeta_q}, \tag{27}$$

allows us to rewrite the efficiency factor in the simplified form,

$$\eta_I(\gamma) = 2\int_0^\infty dx \; x \; e^{-\frac{\gamma}{x}}(1 - e^{-\frac{\gamma}{x}})e^{-\frac{x^2}{2}}. \tag{28}$$

Note that the parameter γ serves as a measure of the adiabaticity of the transition at the crossing point.[12] In Fig. 4, the efficiency factor is plotted as a function of γ. In the small coupling regime, $\gamma \ll 1$, η_I and hence the transition rate increases linearly with the square of the coupling matrix element J as one expects from simple perturbation theory. This corresponds to the nonadiabatic regime investigated by Henry and Lang.[11] However, in the strongly adiabatic regime, $\gamma \gg 1$, the factor η_I approaches zero. Inspection of Fig. 3(a) provides an explanation: as the coupling strength increases, the anticrossing behavior becomes more pronounced, which leads to the reduction in the transition rate.

It is instructive to examine the exponential term contained in Eq. (24) in the high temperature limit. Using Eqs. (20) and (11), we find that this term tends to a thermal activation factor,

$$\exp\left(\frac{-q_1^2}{2\zeta_q^2}\right) \to \exp\left(\frac{-q_1^2}{4S\hbar\omega k_BT}\right) = \exp\left(\frac{-E_A^{D1\to T}}{k_BT}\right)$$

$$(k_BT \gg \hbar\omega). \tag{29}$$

The activation energy barrier $E_A^{D1\to T}$ is shown graphically in Fig. 2(b).

Comparison of Eqs. (24) and (25) in the high temperature limit demonstrates that the forward and reverse transition rates satisfy the detailed balance requirement, $W_I^{T\to D1}/W_I^{D1\to T} = \exp[-\frac{\Delta E_{D1-T}}{k_BT}]$, where $\Delta E_{D1-T} = E_{D1} - E_T$.

It is also instructive to examine explicitly the limiting behavior of the transition rates $W_I^{T\leftrightarrow D1}$ in the limit of zero temperature. Classically, we expect that these rates should tend to zero in this limit, since the crossing point at which the electronic tunneling occurs becomes inaccessible. However, at low temperatures, nuclear tunneling occurs which gives rise to a finite transition rate for $W_I^{D1\to T}$. In this limit, the exponential factor

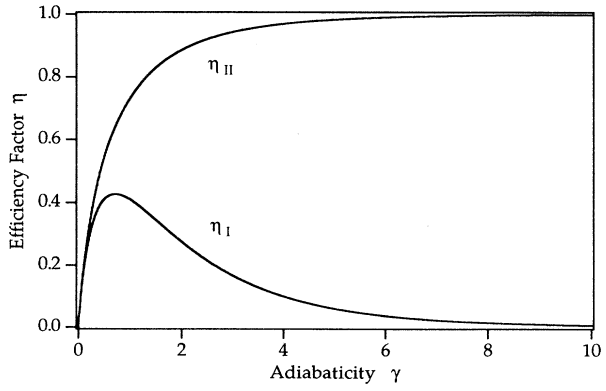

FIG. 4. Dependence of η on the adiabaticity parameter γ.

in Eq. (24) becomes $\exp\left(\frac{-E_A^{D1\to T}}{k_BT^*}\right)$, with k_BT^* given by $\frac{\hbar\omega}{2}\coth\left(\frac{\hbar\omega}{2k_BT}\right)$. At zero temperature then, $k_BT^* = \frac{\hbar\omega}{2}$, the zero-point energy, leading to a finite transition rate, consistent with our quantum mechanical intuition. The expression represents the effect of zero-point fluctuations of the center effectively carrying the system to the crossing point. This interpretation pervades the literature on nonradiative transitions, see for example Englman and Jortner, Ref. 17. However, our expression for the transition rate $W_{\rm I}^{T\to D1}$ is *also* finite in the limit of zero temperature, and thus violates the law of energy conservation. This problem, which is due to a breakdown of the semiclassical approximation inherent in the use of the configuration coordinate decription, has been widely ignored in the literature. Unfortunately, a correct treatment incorporating a fully quantum mechanical description of the nuclear tunneling has not been worked out in the strong electronic coupling regime. Until this problem is solved, the expressions derived here must be regarded as unreliable in the low temperature limit.

2. *Transition rate through q0: Case II*

Having developed expressions for the transition rates between the excited state $D1$ and the trap, T, we now turn to the second type of transition, case II, which characterizes the crossing point $q0$ shown in Fig. 2. We assume in the following that, prior to any crossing phenomena at $q0$, the deep center is fully relaxed and in thermal equilibrium with the surrounding lattice. Thus we neglect processes, e.g., in which an electron is captured at $q1$ by the trap and subsequently transitions at crossing point $q0$ *before* the deep level has cooled — within a timescale of a few vibrational periods.

Reference to Fig. 3 shows that the situation at $q0$ is quite distinct from that of case I. Here, we expect that as the coupling strength increases and the adiabatic limit is reached, the transition rate prefactor should approach $\omega/2\pi$. The reason is that, as the coupling between the quantum dot and the trap is increased, the configuration coordinate diagrams anticross in such a way that the crossing probability approaches unity. The transition rate should, therefore, contain a prefactor which is simply equal to the attempt frequency — the vibrational frequency of the defect. This turns out in fact to be the case. Reasoning analogous to that presented in the last section leads to the expressions

$$W_{\rm II}^{D0\to T} = \frac{\omega}{2\pi}\ \eta_{\rm II}(\gamma)\ \exp\left[-\frac{q_0^2}{2\zeta_q^2}\right], \tag{30}$$

and

$$W_{\rm II}^{T\to D0} = \frac{\omega}{2\pi}\ \eta_{\rm II}(\gamma)\ \exp\left[-\frac{(q_0-2S\hbar\omega)^2}{2\zeta_q^2}\right] \tag{31}$$

for the forward and reverse transition rates between $D0$ and T, respectively (for details see Refs. 12 and 14). The efficiency factor for these transitions is given in terms of the adiabaticity factor γ defined above as

$$\eta_{\rm II}(\gamma) = 2\int_0^\infty dx\ x\ \frac{1-e^{-\frac{\gamma}{x}}}{2-e^{-\frac{\gamma}{x}}}\ e^{-\frac{x^2}{2}}. \tag{32}$$

This relation is plotted in Fig. 4. To derive this expression, note that the total crossing probability in case II is not $P = 2R(1-R)$, as in Eq. (14) corresponding to case I, but rather

$$P = 2\frac{1-R}{2-R}. \tag{33}$$

To see this, note that in case II, the electron crosses from the first state (e.g., state T) to the second (e.g., state $D0$), during the first passage through q_0 with probability $1-R$, with no probability of reemission: once in the second state the system is assumed to thermalize. The second possibility is that the electron does not cross over during the first passage (probability R), but does so in the second (with probability $1-R$), and remains in the second state during the third passage (probability R). However, if the electron crosses back again during the third passage, it remains hung up in a local minimum in the vicinity of the crossing point $q0$, so that we must continue to add up the contributions of higher order processes. Continuing in this way, the total probability of a transition is

$$P = (1-R) + R[(1-R)R + (1-R)^3R + (1-R)^5R + \cdots],$$

which sums to Eq. (33).

As in case I, the transition rate increases as the square of the electronic matrix element, J, in the limit of weak interaction.[12] As we expect on physical grounds, the efficiency factor approaches unity in the adiabatic regime.

As before, these expressions in the high temperature limit take the thermally activated forms,

$$W_{\rm II}^{D0\to T} = \frac{\omega}{2\pi}\ \eta_{\rm II}(\gamma)\exp\left[-\frac{E_A^{D0\to T}}{k_BT}\right] \quad (k_BT \gg \hbar\omega), \tag{34}$$

$$W_{\rm II}^{T\to D0} = \frac{\omega}{2\pi}\ \eta_{\rm II}(\gamma)\exp\left[-\frac{E_A^{T\to D0}}{k_BT}\right] \quad (k_BT \gg \hbar\omega). \tag{35}$$

$E_A^{D0\to T}$ and $E_A^{T\to D0}$ are activation energies for emission from the quantum dot to the trap, shown graphically in Fig. 2(b). Again the high temperature rates satisfy the detailed balance requirement, $W_{\rm II}^{D0\to T}/W_{\rm II}^{T\to D0} = \exp[\frac{\Delta E_{D0-T}}{k_BT}]$, where $\Delta E_{D0-T} = E_{D0} - E_T$.

To this point in the discussion, we have applied Sumi's formalism[12,13] to the description of transitions between a quantum dot and a deep level, lumping all of the details of the interaction into one parameter, the electronic matrix element, J. We turn, in the next subsection, to a discussion of this quantity.

D. Hopping integral

The interaction between the quantum dot and the deep level is treated here in the tight-binding approximation, which is appropriate if the density of quantum dots and deep levels is sufficiently low. We take the wave function of the isolated trap to be $|T\rangle$, given previously in Eq. (3). Bound levels of the isolated quantum dot are denoted $|Dl\rangle$. Each of the $2l+1$ degenerate states in level l have coordinate representations, $\psi_{l,m}(\vec{\rho})$, where the angular momentum subscript $l = 0, 1$ identifies the ground and first excited levels of the quantum dot, respectively. We take the quantization axis to lie along the line joining the quantum dot to the deep level (Fig. 1). Note that only states with $m = 0$ couple to the trap. The envelope wave functions may be readily calculated in the effective mass approximation, see for example Ref. 18. The result for a spherical quantum dot of radius R is

$$\langle\vec{\rho}|D_l\rangle = \psi_{l,m}(\vec{\rho}) = A_{l,m}\ j_l(k\rho)\ Y_l^m(\Omega) \qquad (\rho < R),$$

$$\langle\vec{\rho}|D_l\rangle = \psi_{l,m}(\vec{\rho}) = A_{l,m}\ h_l(i\kappa\rho)\ Y_l^m(\Omega) \qquad (\rho > R), \tag{36}$$

where wave number k is related to the energy of the state through $E_{l,m} = \frac{\hbar^2 k^2}{2m^*}$ and the wave number κ outside the quantum dot is determined by the usual condition of continuity of the particle current, namely, that $[1/m^*][d\psi/d\rho]$ be continuous.

It can be readily shown that at crossing points on the configuration coordinate diagram, the *electronic* energy of the trap and the corresponding quantum-dot state are degenerate. Thus, in the vicinity of the crossing point, we can write the electronic wave function of the coupled system as a superposition of the two nearly degenerate states,

$$|\phi\rangle = a|Dl\rangle + b|T\rangle. \tag{37}$$

In this case, the hopping matrix element can be written

$$J = \langle Dl|H|T\rangle = \langle Dl|H_T|T\rangle + \langle Dl|V_{\rm QD}|T\rangle, \tag{38}$$

where H_T represents the Hamiltonian of the *isolated* deep level and $V_{\rm QD}$ is the potential well comprising the quantum dot. Note that we have assumed orthogonality between the states corresponding to the isolated quantum dot and deep level. This assumption is justified for sufficiently large separation. Since at a crossing point the electronic energy of the deep state and the quantum dot are degenerate, the last expression further simplifies to

$$J = E_{Dl}\langle Dl|T\rangle + \langle Dl|V_{\rm QD}|T\rangle. \tag{39}$$

This form is particularly appealing since the trap potential does not appear. The hopping matrix element only depends on the structure of the quantum dot and the overlap between the electronic wave functions of the dot and trap. The latter is determined predominantly by the decay of the wave functions in the barrier region separating the quantum dot and the deep level, lending confidence to our use of the effective mass approximation in this problem. In the following section, we present results of an illustrative numerical calculation of the transition rates between a quantum dot and a deep-level trap made using the results presented in this section and in Sec. II C.

III. NUMERICAL CALCULATIONS

We consider the system depicted in Fig. 1 consisting of a spherical $In_xGa_{1-x}As$ quantum dot of radius R embedded in a GaAs matrix, coupled to a deep-level trap located a distance A from the center of the quantum dot. Spherical symmetry is assumed for numerical simplicity. In order to maximize the pertinence of the calculation to experiments reported in the literature,[6,7] we have used $In_xGa_{1-x}As$ band structure parameters and band offsets found for $In_xGa_{1-x}As$ quantum wells coherently strained to GaAs, which were reported in Ref. 19. These parameters, derived for $In_xGa_{1-x}As$/GaAs quantum wells, therefore, are appropriate to a condition of uniaxial rather than hydrostatic strain. Strictly speaking, a spherical InGaAs quantum dot would be expected to be isotropically strained to the surrounding GaAs material. We have chosen, however, to use the parameters appropriate for uniaxial strain since in actual experiments,[6,7] $In_xGa_{1-x}As$ quantum dots formed by the coherent islanding technique have been found to possess a plateletlike morphology more adequately described by a condition of uniaxial strain. To reproduce the energy of the observed quantum-dot photoluminescence band [$\hbar\omega \approx 1.15$ eV, (Ref. 6)], we take the dot radius to be 5 nm and assume an indium mole fraction $x = 0.5$.

For this choice of parameters, there are two bound conduction-band states in the quantum dot — $|D0\rangle$, the ground state with a calculated binding energy of 192 meV, and $|D1\rangle$, an excited state with a binding energy of 25 meV. These parameters are reflected in Fig. 2. Since the binding energy of $D1$ is less than the longitudinal-optical phonon energy (36 meV), this state is assumed to be thermalized.[2] However, LO-phonon scattering between the ground state of the quantum dot and either the excited state or continuum states above the barrier is assumed to be suppressed due to the bottleneck effect.

A. Parameters associated with the deep level

In our model calculation, we chose as a representative deep center the electron trap $M1$, which is commonly observed in n-type GaAs grown by molecular beam epitaxy under arsenic stabilized conditions.[9,10] This trap has thermal activation energy of emission of 0.19 eV and an emission cross section $\sigma \approx 10^{-14}$ cm^{-2}.[9] Since the capture barrier associated with this defect has not been measured, the lattice relaxation energy $S\hbar\omega$ is not known. We therefore assume a value $S\hbar\omega = 100$ meV, which is typical for electron traps in GaAs, such as $M3$ and $E3$.

This gives a capture barrier of 20 meV, consistent with the upper limit of 24 meV estimated in Ref. 10. The vibrational frequency, ω, associated with the defect is chosen so that $\hbar\omega = 10$ meV. This choice corresponds to the transverse-acoustic peak in the phonon density of states.[20] The electronic energy and the configuration coordinate diagram calculated with these parameters are depicted in Fig. 2.

B. Transition rates

The results of the tight-binding calculation of the hopping integral J, made using Eq. (39), are plotted in Fig. 5 as a function of the spatial separation between the quantum dot and the deep level. The two curves shown in Fig. 5 correspond to transitions occurring at crossing points $q1$ and $q0$, which, respectively, describe coupling between the excited state of the quantum dot and the trap, $D1-T$, and between the trap and the quantum-dot ground state, $D0-T$. As expected, the hopping integrals decrease exponentially with separation at large distances. However, the figure clearly shows that the tight-binding approximation breaks down at small distances, particularly for the coupling $D1-T$. For separations less than approximately 10 nm, the hopping integral for $D1-T$ calculated with Eq. (39) becomes comparable to the binding energy of T and $D1$, providing a clear indication that the tight-binding approximation is breaking down. An indication of the cause is provided by examination of the inset of Fig. 5, which shows that the overlap integrals $\langle Di|T\rangle$ for $i = 0, 1$ are sizable at small separations, violating our assumption of orthogonality. However, correction for the lack of orthogonality would further *increase* the hopping term. In actuality the most significant error made here in the calculation of J is the neglect of coupling to the continuum states lying in energy above the barrier.

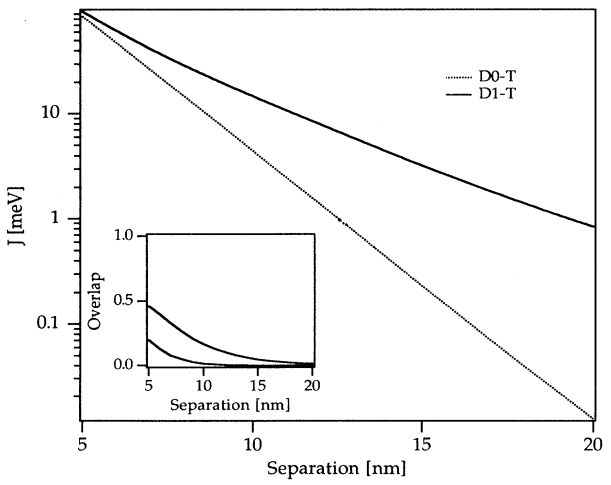

FIG. 5. Hopping integral for the transitions $D0 \leftrightarrow T$ and $D1 \leftrightarrow T$ plotted versus separation between trap $M1$ and quantum dot. The inset shows the overlap integrals $\langle D0|T\rangle$ and $\langle D1|T\rangle$ versus separation.

The effect of such coupling is to reduce the magnitude of the effective hopping term. To account for this quantitatively is rather difficult. Fortunately, it is unnecessary to do this to establish qualitative trends, which is the primary aim in this paper.

The transition rates calculated using Eqs. (24), (25), (30), and (31) are shown in Fig. 6, at room temperature, part (a), and at liquid helium temperature, part (b). The transition rates are plotted as a function of the separation between the quantum dot and the deep level. Figure 6(a) shows that at room temperature, the rate of multiphonon-assisted tunneling of electrons out of the relaxed trap into the ground state of the quantum dot, $T \rightarrow D0$, exceeds 10^9 s^{-1} for separations as large as 15 nm. The reverse rate is not distinguishable from the forward rate in the figure owing to the closeness in energy of the trap energy E_T with E_{D0}. As the separation is reduced, the tunneling rate approaches 10^{12} s^{-1}. This is easily understood by reference to Figs. 3 and 4 and Eq. (25). As the coupling between the quantum dot and the trap is increased, the transition becomes increasingly

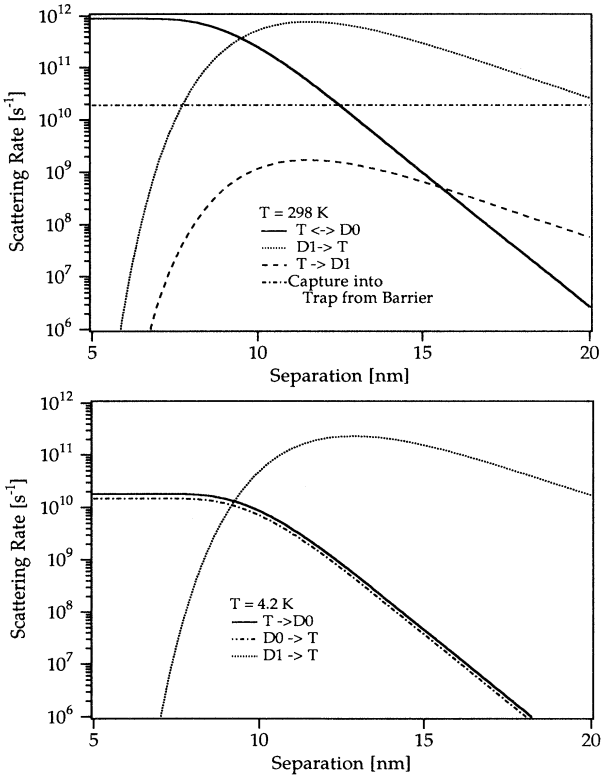

FIG. 6. Scattering rates versus separation between quantum dot and deep level. The calculation is performed for a 5 nm radius $In_{0.5}Ga_{0.5}As/GaAs$ quantum dot and the deep-level trap $M1$. (a) Temperature 298 K. Rates shown are for the transitions $D1 \leftrightarrow T$ and $T \leftrightarrow D0$. Also shown is the direct capture rate for unbound electrons into the trap. (b) Temperature = 4.2 K. The direct capture rate and the rates corresponding to the transition $T \rightarrow D1$ do not appear on the scale of the figure.

adiabatic. In the adiabatic limit, the configuration coordinate diagrams anticross, Fig. 3, so that the crossing probability and the efficiency factor η_{II} approach unity. The transition rate thus tends to $\omega/2\pi$, the vibrational frequency of the deep center, which serves as an attempt frequency. The transition rate for the process $D1 \rightarrow T$ is appreciably higher at large separation than that of $T \rightarrow D0$. This is expected since in the limit of weak coupling the transition rate depends linearly on the coupling parameter γ, which is larger for the transition $D1 \rightarrow T$. However, at small separations, the transition rates for the processes $D1 \leftrightarrow T$ behave qualitatively differently from $D0 \leftrightarrow T$: the rates for $D1 \leftrightarrow T$ reach a maximum as the separation is reduced (coupling is increased) and subsequently fall off with decreasing separation. This somewhat counter-intuitive feature is explained by reference to Figs. 3 and 4. As the coupling is increased, the anticrossing behavior at $q1$ is accentuated, causing the reduction in the calculated tunneling rate. However, while the reduction in the transition rate with decreasing separation in Fig. 6 is *qualitatively* correct, the quantitative behavior is not. As discussed in the preceeding paragraph, the simple tight-binding model used here breaks down at small separations and causes an overestimate of the hopping integral. Thus, the curves corresponding to the transtion $D1 \rightarrow$ and the reverse process quantitatively underestimate the transition rates for separations less than $\approx$ 10 nm. Finally, note that the transition rate for the process, $T \rightarrow D1$ is substantially lower than that of $D1 \rightarrow T$, owing to the different activation barriers for the two processes [see Fig. 2(b)].

Also shown in Fig. 6(a) is the *direct* capture rate from the barrier into the trap, given by Eq. (1), assuming an electron concentration of 10^{17} cm^{-3} in the GaAs barrier. The sum of this rate and that of $D1 \rightarrow T$ exceeds 10^{10} s^{-1} for all separations up to 20 nm. Meanwhile, the transition rate from the trap to $D0$ exceeds 10^{10} s^{-1} for separations less than 12 nm. We therefore conclude that, *if the situation depicted in Fig. 1 were to be physically realized* with a defect $M1$ within 12 nm of an $In_xGa_{1-x}As$ quantum dot, the relaxation rate into the quantum-dot ground state from the barrier would exceed 10^{10} s^{-1} at room temperature. Thus, no bottleneck effect would be observed, and the luminescence efficiency of the quantum dot would not be degraded by slow relaxation. These conclusions are qualitatively true even at liquid helium temperature, Fig. 6(b). There, we see that the rate of transition from the trap into the ground state of the quantum dot exceeds 10^{10} s^{-1} for separations out to 10 nm, more than sufficient to overcome the bottleneck effect. The rate of capture into the trap drops below 10^{9} s^{-1} below 8 nm, but this rate is underestimated here due to the tight-binding approximation used, as described above.

IV. CONCLUSIONS

Given the interesting result that coupling between a deep level and a quantum dot can reduce intraband relaxation times in the dot to less than 100 ps, an obvious question emerges concerning the likelihood of this situation arising in an experiment. The defect $M1$, which we chose for the purpose of illustration, is known to occur in MBE-grown GaAs and is thought to consist of a defect-impurity complex involving arsenic vacancies.[10] However, in modern MBE reactors the concentration of this trap is typically very low, $\approx 10^{12}$ cm^{-3}. According to the preceeding discussion, for the defect to provide a rapid relaxation pathway, it must lie roughly within a spherical volume of 10 nm radius centered on a quantum dot. The resulting probability of interaction of an $In_xGa_{1-x}As$ quantum dot embedded in well-grown MBE GaAs is only of the order 10^{-5}, which is not encouraging. However, this estimate assumes that the concentation of traps is as low as in the best MBE-grown quantum wells, and that the distribution is uniform and in particular, *uncorrelated with the position of the quantum dots.* This is unlikely to be the case. It is possible that quantum-dot fabrication steps lead to the production of point defects and *migration* to the vicinity of the quantum dot. One such mechanism is migration of native defects in a strain field. For example, it has been observed that vacancies and interstitials migrate, respectively, to regions of maximum and minimum compression in $GaAs/Al_xGa_{1-x}As$ laser diode structures.[21] This phenomenon, together with the fact that strain gradients certainly exist in $In_xGa_{1-x}As/GaAs$ quantum dots produced by the coherent islanding technique[6–8] is highly suggestive. Indeed, recent time-resolved measurements of photoluminescence in these samples failed to reveal a significant bottleneck effect,[7] in contradiction with theoretical expectations for an ideal quantum dot.[1–5] The lack of a significant bottleneck effect is consistent with the phenomena described here pertaining to quantum dots coupled to deep levels. Experiments to characterize the distribution of electron traps would thus be highly interesting. Finally, the physical process described here is not specific to the defect $M1$ — it is conceivable that trap-forming impurities could be used to intentionally dope a quantum-dot sample, so as to provide energy-relaxation channels.

ACKNOWLEDGMENTS

I thank Howard Carmichael, Roger Haydock, and Michael Raymer for stimulating discussions regarding various aspects of this project. I am grateful to Michael Raymer for alerting me to the energy conservation problem discussed in Sec. II C. I thank David Griffiths and Darrell Schroeter for critical reading of the mansuscript. This material is based upon work supported by the National Science Foundation under Grant No. DMR 9304537. Support by the Oregon Joint Centers for Graduate Schools in Engineering is gratefully acknowledged.

[1] U. Bockelmann and G. Bastard, Phys. Rev. B **42**, 8947 (1990).
[2] H. Benisty, C.M. Sotomayor-Torres, and C. Weisbuch, Phys. Rev. B **44**, 10 945 (1991).
[3] T. Inoshita and H. Sakaki, Phys. Rev. B **46**, 7260 (1992).
[4] Janet L. Pan, Phys. Rev. B **49**, 2536 (1994).
[5] Janet L. Pan and Peter L. Hagelstein, Phys. Rev. B **49**, 2554 (1994).
[6] D. Leonard, M. Krishnamurthy, C.M. Reaves, S.P. Denbaars, and P.M. Petroff, Appl. Phys. Lett. **63**, 3203 (1993).
[7] G. Wang, S. Fafard, D. Leonard, J.E. Bowers, J.L. Merz, and P.M. Petroff, Appl. Phys. Lett. **64**, 2815 (1994).
[8] J.-Y. Marzin, J.-M. Gerard, A. Izrael, D. Barrier, and G. Bastard, Phys. Rev. Lett. **73**, 716 (1994).
[9] D.V. Lang, A.Y. Cho, A.C. Gossard, M. Ilegems, and W. Weigman, J. Appl. Phys. **47**, 2558 (1976).
[10] P. Blood and J.J. Harris, J. Appl. Phys. **56**, 993 (1984).
[11] C.H. Henry and D.V. Lang, Phys. Rev. B **15**, 989 (1977).
[12] Hitoshi Sumi, J. Phys. Soc. Jpn. **49**, 1701 (1980).
[13] Hitoshi Sumi, Phys. Rev. Lett. **47**, 1333 (1981).
[14] Hitoshi Sumi, J. Phys. Soc. Jpn. **51**, 1745 (1982).
[15] L.D. Landau and E.M. Lifshitz, *Quantum Mechanics* (Permagon Press, Oxford, 1977).
[16] C. Cohen-Tannoudji, B. Diu, and F. Laloe, *Quantum Mechanics* (Wiley, New York, 1977).
[17] Robert Englman and Joshua Jortner, Mol. Phys. **18**, 145 (1970).
[18] Peter C. Sercel and Kerry J. Vahala, Phys. Rev. B **42**, 3690 (1990).
[19] X. Marie, J. Barrau, B. Brousseau, Th. Amand, M. Brousseau, E.V.K. Rao, and F. Alexandre, J. Appl. Phys., **69**, 812 (1991).
[20] J.S. Blakemore, J. Appl. Phys. **53**, R123 (1982).
[21] B. Wakefield and M.J. Robertson, in *Microscopy of Semiconducting Materials, 1981*, edited by A.G. Cullis and D.C. Joy, IOP Conf. Proc. No. 60 (Institute of Physics, London, 1981), p. 447.